THE ASTRONOMICAL JOURNAL VOLUME 85, NUMBER 8 AUGUST 1980

EXTENDED RADIO SOURCES AND ELLIPTICAL GALAXIES. IV. STRUCTURES OF 40 RESOLVED SOURCES

E. B. FOMALONT
National Radio Astronomy Observatory, [a] Charlottesville, Virginia 22901

J. J. PALIMAKA and A. H. BRIDLE
Department of Physics, Queen's University at Kingston, Ontario K7L 3N6, Canada
Received 24 March 1980

ABSTRACT

Partial-synthesis maps are presented for a sample of extended radio galaxies at 2.7 and 8.1 GHz. These maps were used to determine the overall sizes, orientations, and gross morphologies of the sources during a study of the relative orientations of extended radio sources and their parent elliptical galaxies. The optical identifications of 13 sources have been confirmed by the detection of small-diameter radio components within their parent galaxies. Two radio galaxies in this group—0238+085 and 1250−102—have extended radio cores and elongated structures suggestive of two-sided radio jets similar to those of 3C449, NGC 315, and 3C31. The spectrum-luminosity relation found for extended radio cores in Paper I of this series has been confirmed using spectral indices of improved accuracy.

I. INTRODUCTION

The work described in this series of papers is directed toward understanding the relationship between the physical characteristics of the extended radio structures of elliptical radio galaxies and (a) the orientation of these structures relative to their parent galaxies and (b) the characteristics of radio "cores" within the optical boundaries of the parent galaxies. In this paper we present the results of observations of 40 radio sources using the NRAO 4-element interferometer at 2.7 and 8.1 GHz. These sources were encountered (but not necessarily finally used) in studies of the relative orientations of radio sources and their parent galaxies by Palimaka *et al.* (1979) (hereafter referred to as PBFB). In general, the maps in the present paper either show more detail than previous published maps of these sources or are the first high-resolution maps available.

The sources are a subset of a sample of ~500 radio galaxies which were observed at Green Bank using a partial synthesis technique, i.e., visibility data were obtained from observations at a small number of hour angles using (so far as possible) only those interferometer spacings which contained information at angular scales appropriate to the source being observed. The selection of the overall sample and the observing and data-reduction procedures were described in detail by Bridle and Fomalont (1978) (Paper I).

Optical positions of the centers of galaxies were measured to confirm the identifications of sources used in this work; these positions are given by Goodson *et al.* (1979) (Paper III) and by Palimaka *et al.* (1980) (Paper V; following paper). Paper VI (in preparation) will present results from the radio-optical orientation studies and will discuss their implications for models of energy transport in extended extragalactic radio sources.

II. RESULTS

Figures 1 through 7 present contour maps for 39 sources; 2.7-GHz maps are shown unless the source is $\lesssim$30 arcsec in angular size or unless the 8.1-GHz data were found to contain significantly more information on source structure. Maps at both frequencies are included for the source 1000+201, for which there is a disagreement of ~15° between the apparent orientations of the major axis at 2.7 and 8.1 GHz. It is possible that this source has structural complexity that is not well represented in our maps and that full synthesis observations are necessary to map this source satisfactorily.

No map is given for the source 0325+023, since our 2.7-GHz map showed no more detail than did that at 1.4 GHz by Fomalont (1971). The source is included in this paper since we did detect a small-diameter radio component which confirms the optical identification (see Tables I and II).

In several of the maps in Figs. 1 to 7 the symbol "+" is used to indicate the position of a small component which has been subtracted from the map (as described in Paper I, Sec. III b) in order to show the fainter extended structure more clearly. The positions of small components which were not subtracted before mapping and/or the positions of the optical identifications are indicated in Figs. 1 to 7 by the "×" symbols.

Table I has entries for 40 sources describing the radio

[a] Operated by Associated Universities, Inc., under contract with the National Science Foundation.

 0004-6256/80/080981-14$00.90

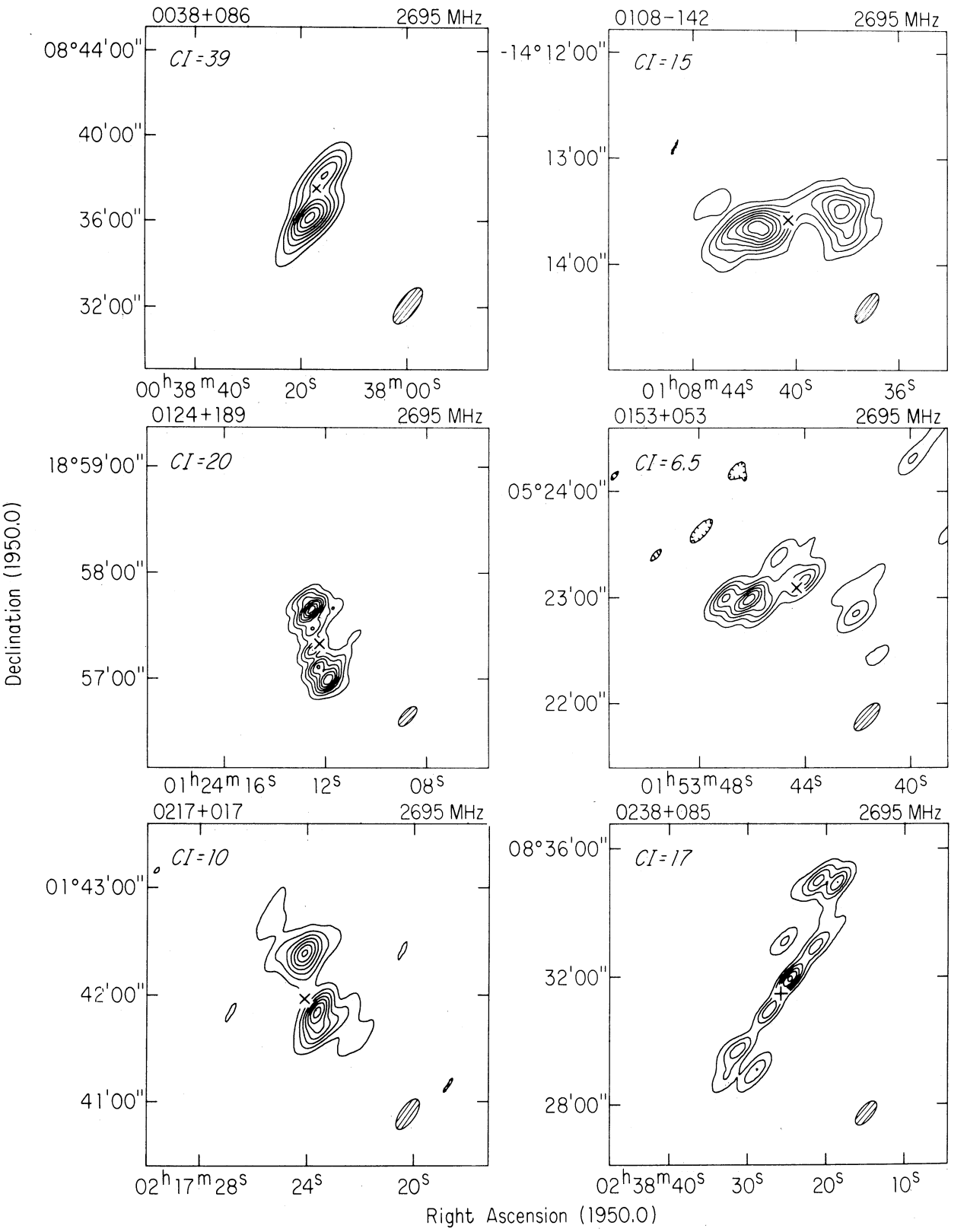

FIG. 1. Contour maps representing the extended structures of the sources. The contour interval is given in the upper left-hand corner in units of mJy/beam area. The FWHM of the "clean" beam is shown by the cross-hatched ellipse at the lower right of each map.

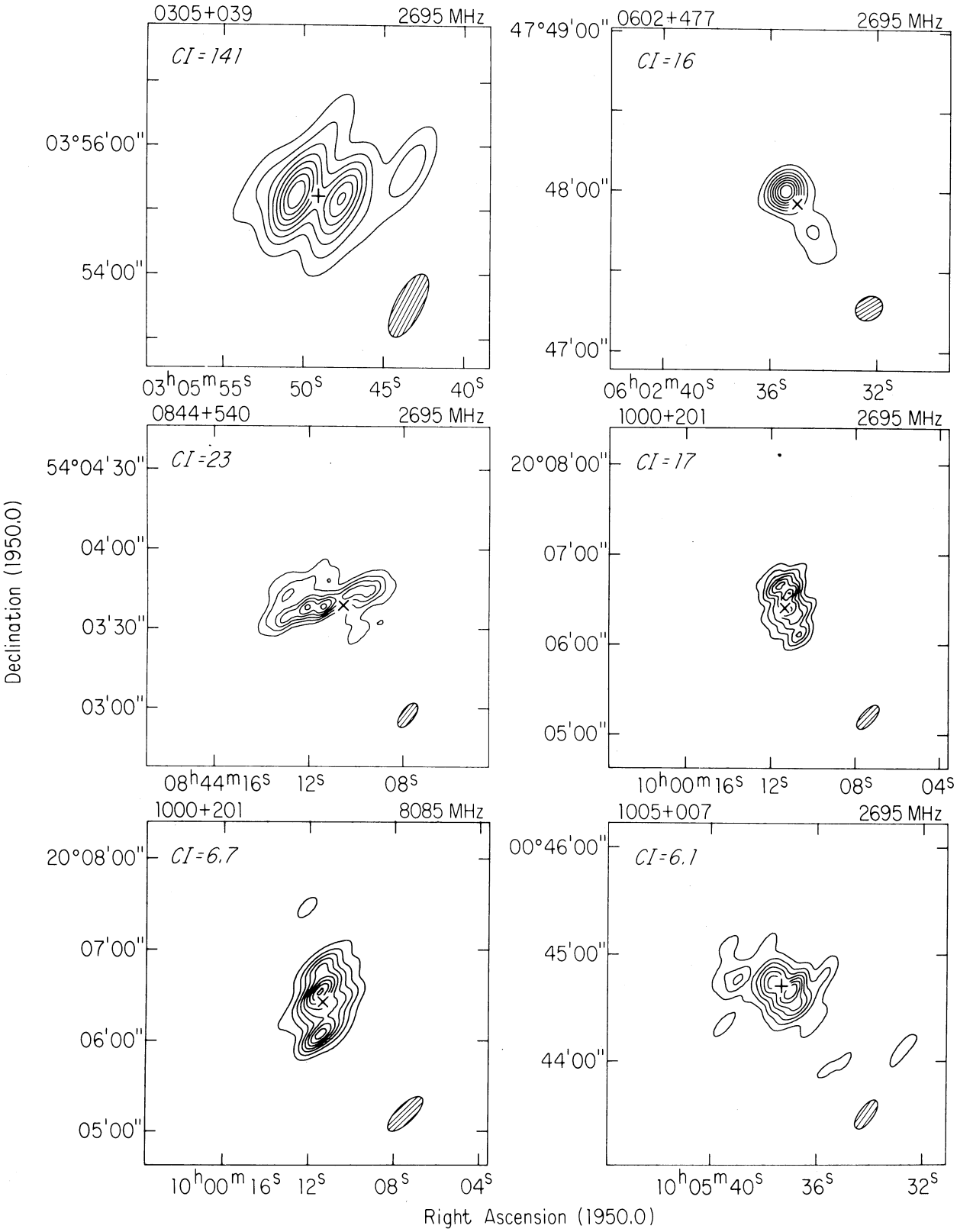

FIG. 2. Same as Fig. 1.

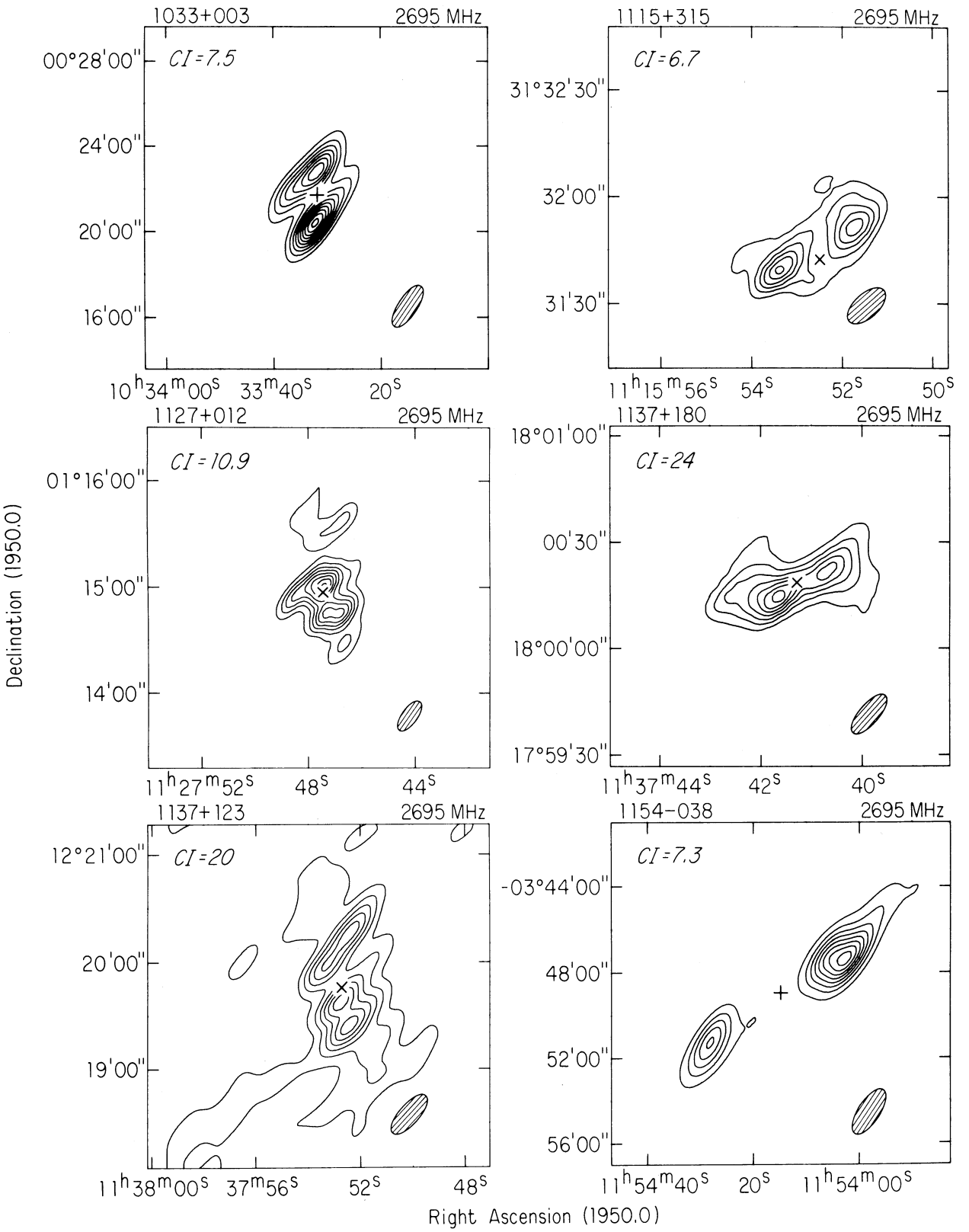

FIG. 3. Same as Fig. 1.

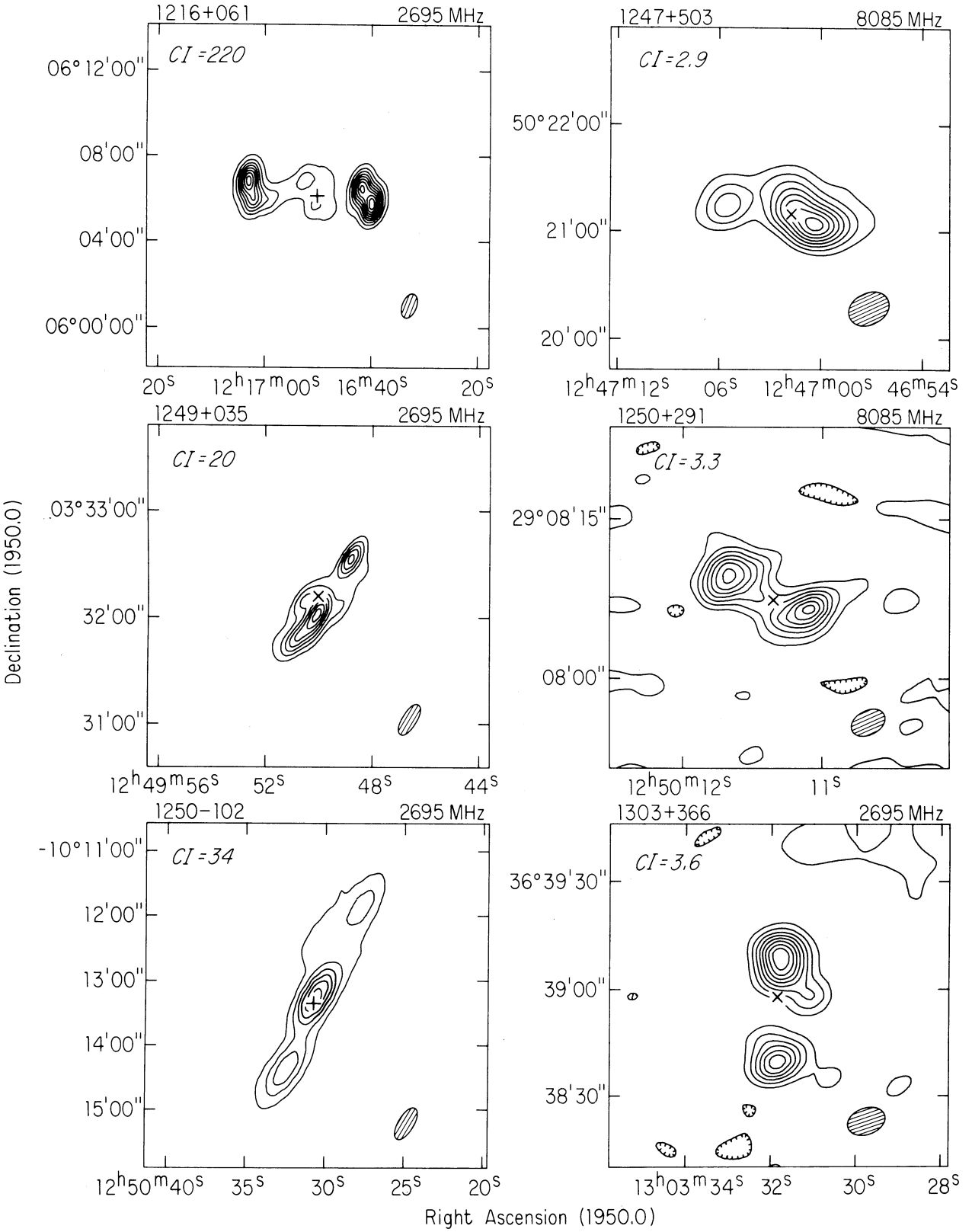

FIG. 4. Same as Fig. 1.

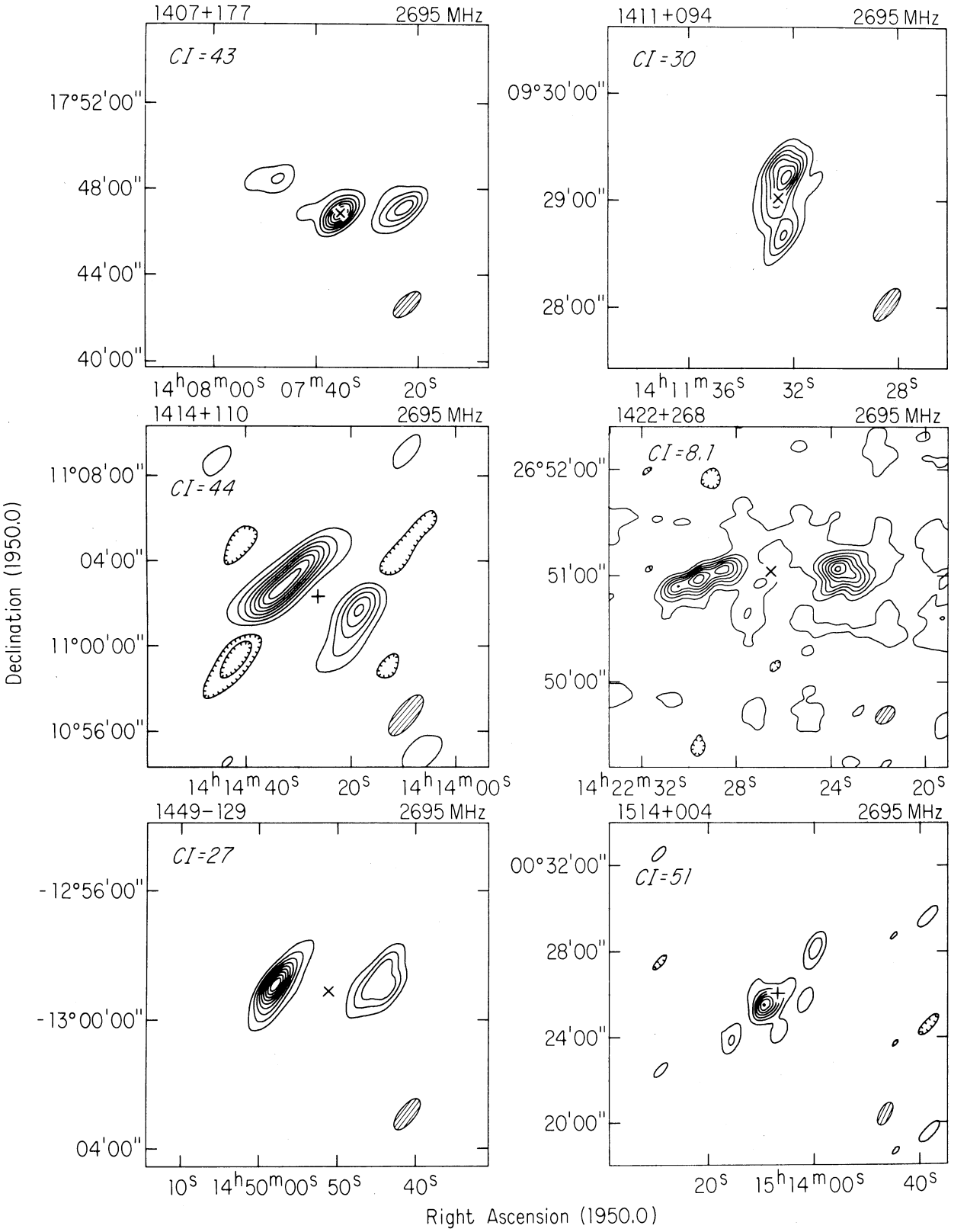

FIG. 5. Same as Fig. 1.

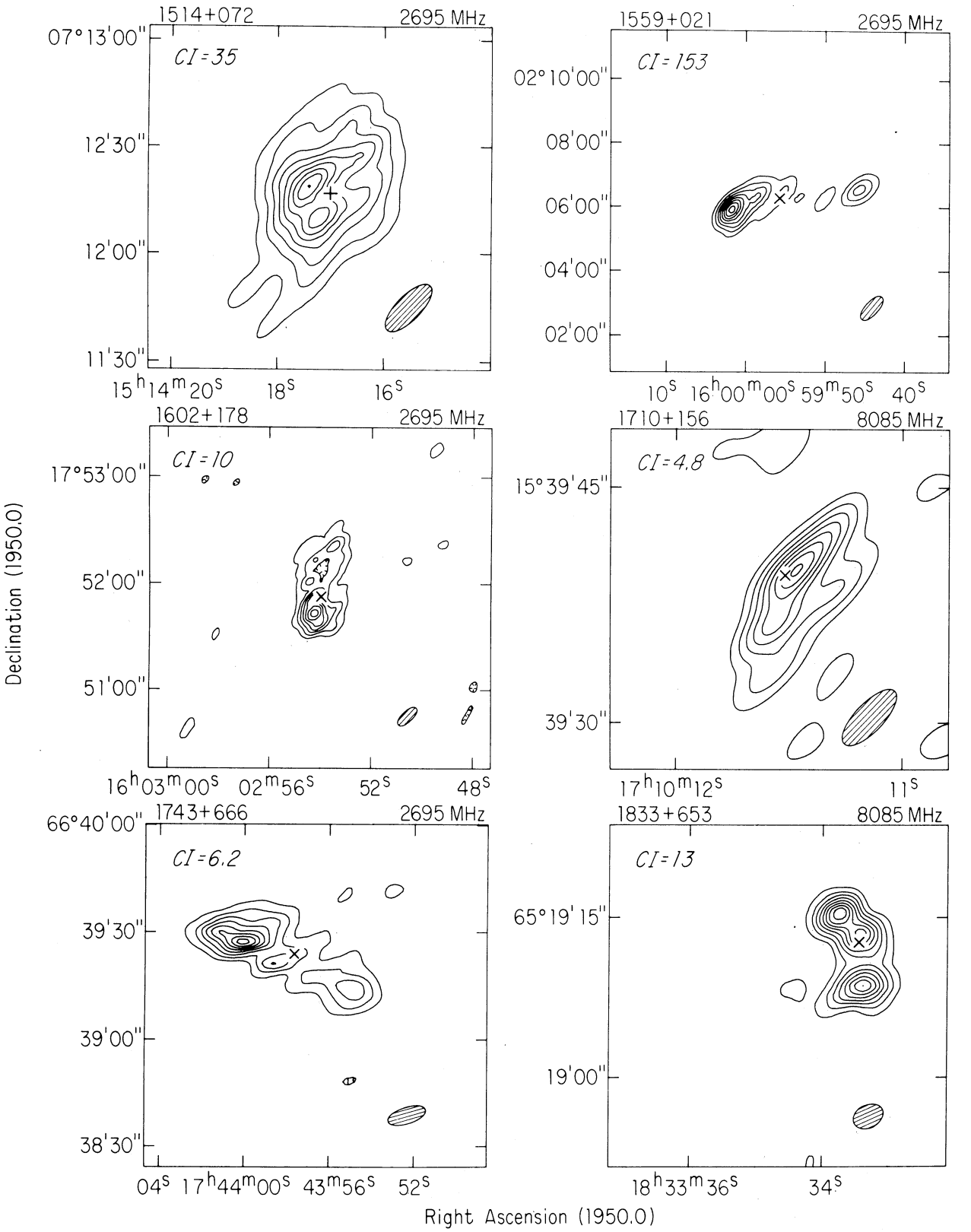

FIG. 6. Same as Fig. 1.

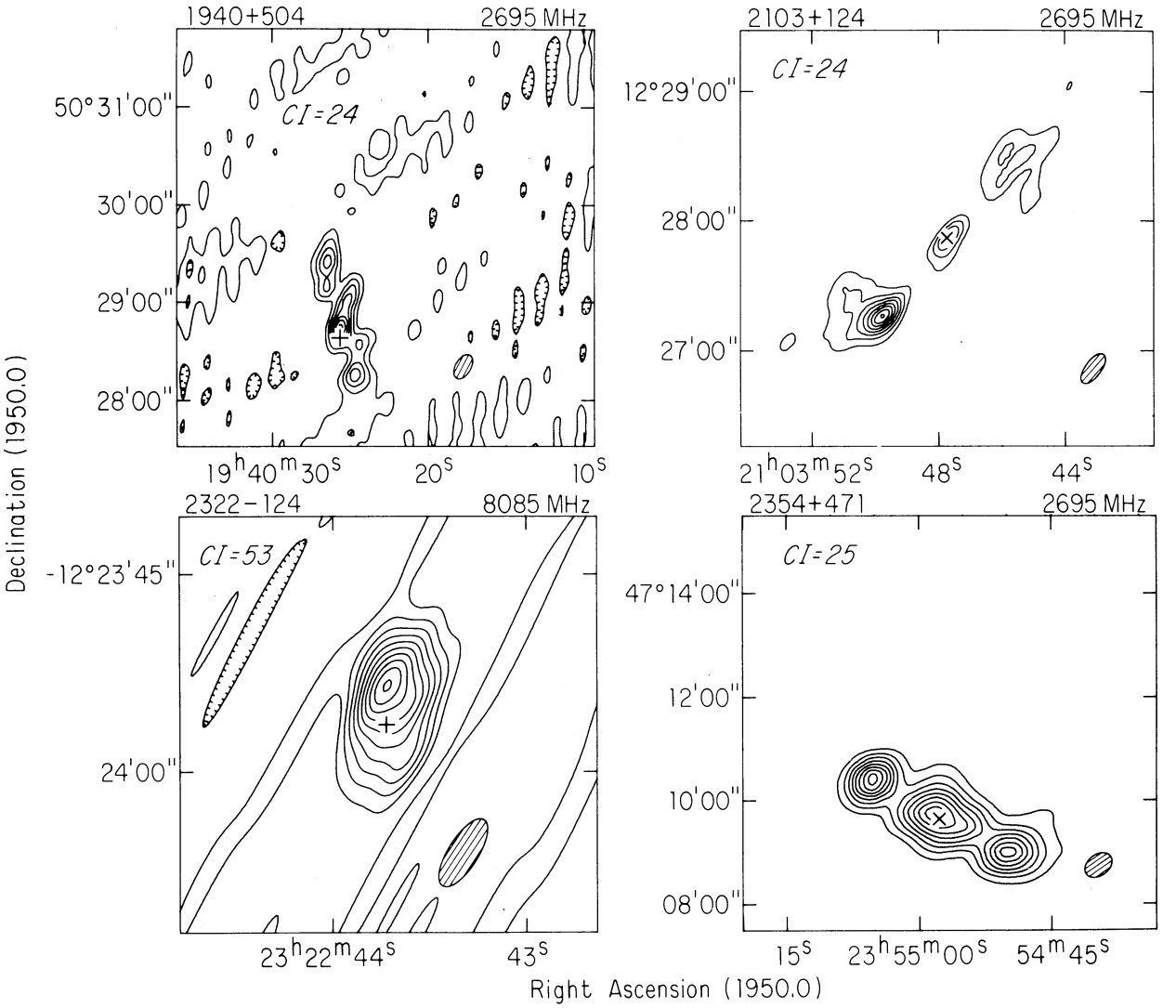

FIG. 7. Same as Fig. 1.

characteristics of their extended structures and their relations to their optical identifications. Column 1 gives the radio source name in the IAU convention (upper line) and a common name (nomenclature as in Kesteven and Bridle 1977) from a radio source catalog (lower line). Columns 2 and 3 list the 1950.0 radio positions (upper line) and the 1950.0 positions of the optical identifications (lower line). The radio position is either that of a small-diameter "core" within the extended structure (in which case letter S appears in column 4) or that of the radio centroid (letter C in column 4). The positions of the centroids were calculated from the positions and flux densities of sets of Gaussian components fitted to our radio visibility data.

Column 5 classifies the overall radio structure of each source using an extension of the scheme introduced in Paper I. Schematic maps for the classes of structure encountered in this paper are shown in Fig. 8. By analogy with our classification for the extended features of T (triple) and C (core-halo) sources with central components, we classify as D (double) or E (elongated), respectively, those structures in which a core component has not been detected. The classes C and E are applied to sources where the extended emission is not clearly, or uniquely, bifurcated.

Column 6 (upper line) gives the integrated 2.7-GHz flux density of each source. This is normally taken from our pencil-beam observations with the NRAO 91-m telescope (Paper I, Sec. II b), but if the interferometer data show a confusing source within the beam of the 91-m telescope, the flux density is taken from a model that was fitted to the field using data from the shortest interferometer spacings (<300 m). For a few very extended sources the integrated flux density was taken from observations with the NRAO 43-m telescope.

The lower line of column 6 gives the percentage of the

TABLE I. Radio parameters of the 40 sources.

SOURCE NAME	RADIO/OPTICAL POSITION R.A. (1950.0)	DEC.	ID TYPE	RADIO CLASS	S(2.7) Jy	LAS arcsec	RADIO P.A.	NOTES REFS.
0038+086	$00^h38^m17^s.60$	$+08^\circ36'43''.0$	C	D	0.70	180	165± 4°	1
PK0038+08	17.10 ±0.30	37 34.0 ±5.0			100%			unpub
0108-142	01 08 39.83	-14 13 32.3	C	D	0.90	90	100± 5	
PK0108-142	40.30 ±0.10	35.8 ±0.4			100%			Pal80
0124+189	01 24 12.32	+18 57 19.6	C	D	0.92	60	13± 5	2
PK0124+18	12.24 ±0.02	19.1 ±0.4			100%			Pal80
0153+053	01 53 44.46	+05 23 01.7	C	D	0.49	85	84±10	3
PK0153+05	44.31 ±0.04	05.4 ±0.4			67%			Pal80
0217+017	02 17 24.00	+01 42 05.0	C	D	0.35	62	16± 6	4
PK0217+01	24.10 ±0.30	41 58.0 ±5.0			97%			unpub
0238+085	02 38 26.01 ±0.18	+08 31 26.8 ±1.2	S	T	0.80	450	144± 5	5
PK0238+08	25.85 ±0.02	29.0 ±0.4			85%			Pal80
0305+039	03 05 49.08 ±0.03	+03 55 13.5 ±0.4	S	T	5.10	98	56±11	6,7
3CR78	49.08 ±0.04	13.2 ±0.6			94%			Pal80
0325+023	03 25 18.16 ±0.02	+02 23 20.7 ±0.3	S	T	2.98	240	63± 3	8,9,10
3CR88	18.19 ±0.02	20.3 ±0.4			85%			Pal80
0602+477	06 02 35.10	+47 47 55.0	C	D	0.27	30	33± 5	11
4C47.19	35.05 ±0.03	55.2 ±0.6			97%			Pal80
0844+540	08 44 11.29	+54 03 41.0	C	E(D)	1.07	48	113± 5	12
4C54.17	10.49 ±0.04	39.0 ±0.5			100%			Goo79
1000+201	10 00 11.21	+20 06 29.3	C	E(D)	0.67	48	8±10	7,13
PK1000+20	11.33 ±0.02	24.2 ±0.5			100%			Goo79
1005+007	10 05 37.34 ±0.03	+00 44 42.5 ±0.4	S	C(T)	0.34	50	71±10	14,15
PK1005+007	37.34 ±0.03	42.0 ±0.7			94%			Pal80
1033+003	10 33 32.60	+00 21 18.0	C	D	0.35	175	8±11	16
PK1033+003	31.93 ±0.04	41.1 ±0.4			81%			Pal80
1115+315	11 15 52.57	+31 31 45.4	C	D(T)	0.18	30	118± 4	17
B21115+31B	52.50 ±0.03	42.4 ±0.5			79%			Goo79
1127+012	11 27 47.20	+01 15 04.0	C	D	0.46	65	12± 8	18
PK1127+012	47.51 ±0.02	14 56.6 ±0.4			100%			Pal80
1137+180	11 37 41.40	+18 00 18.0	C	D	0.77	40	118± 5	
4C17.52	41.30 ±0.20	18.0 ±3.0			96%			Wil76
1137+123	11 37 53.00	+12 19 47.0	C	D	0.80	90	12± 6	19
PK1137+12	52.64 ±0.02	46.0 ±0.4			100%			Pal80
1154-038	11 54 14.78 ±0.04	-03 48 59.3 ±0.6	S	T	0.30	630	122± 4	7
PK1154-038	14.73 ±0.02	58.9 ±1.1			93%			Pal80
1216+061	12 16 50.00 ±0.03	+06 06 08.4 ±0.3	S	T	12.60	498	83± 7	9,20
3CR270	50.02 ±0.03	08.5 ±0.5			93%			Gri63
1247+503	12 47 01.90	+50 21 07.0	C	E(D)	0.14	70	80± 4	21
WK301	01.68 ±0.04	09.0 ±0.4			(71%)			Pal80

TABLE I. (continued)

SOURCE NAME	RADIO/OPTICAL POSITION R.A. (1950.0)	DEC.	ID TYPE	RADIO CLASS	S(2.7) Jy	LAS arcsec	RADIO P.A.	NOTES REFS.
1249+035	$12^h49^m50^s.00$	+03° 32′ 03″.0	C	D	0.57	77	146± 4°	
PK1249+035	50.00 ±0.40	12.0 ±6.0			100%			Mer70
1250+291	12 50 11.37	+29 08 07.8	C	D	0.28	13	68± 9	
5C4.6	11.35 ±0.05	07.4 ±0.3			(100%)			Goo79
1250−102	12 50 30.70 ±0.05	−10 13 20.5 ±2.0	S	T	0.64	195	162± 6	7
PK1250−10	30.64 ±0.02	21.7 ±1.4			97%			Pal80
1303+366	13 03 31.77	+36 38 56.8	C	D	0.09	44	178± 3	22
B21303+36B	31.83 ±0.02	56.1 ±0.4			97%			Pal80
1407+177	14 07 32.40	+17 47 14.0	C	D	0.80	440	73± 6	23
PK1407+17	34.82 ±0.05	46 52.5 ±0.7			100%			Ghi77
1411+094	14 11 32.30	+09 29 05.0	C	E(D)	0.72	63	178± 5	
PK1411+09	32.55 ±0.03	01.7 ±0.5			100%			Wil73
1414+110	14 14 26.36 ±0.03	+11 02 18.6 ±0.3	S	T	2.70	300	65±20	24,25
3CR296	26.37 ±0.03	19.3 ±0.4			92%			Pal80
1422+268	14 22 26.51 ±0.04	+26 51 02.3 ±0.5	S	T	0.51	120	96± 4	26
B21422+26	26.50 ±0.03	01.8 ±0.4			100%			Pal80
1449−129	14 49 51.50	−12 58 49.0	C	D	0.75	250	89± 5	10,27
PK1449−13	51.00 ±0.30	59 06.0 ±5.0			100%			unpub
1514+004	15 14 06.70 ±0.04	+00 26 01.7 ±0.7	S	T	1.80	355	135± 5	7,9
PK1514+00	06.73 ±0.02	01.5 ±0.4			89%			Pal80
1514+072	15 14 17.01 ±0.02	+07 12 16.6 ±0.5	S	T(C)	2.08	45	15±17	24
3CR317	17.00 ±0.03	16.7 ±0.5			100%			Gri63
1559+021	15 59 57.20	+02 06 09.2	C	D(T)	5.00	300	99± 4	9,28
3CR327	55.67 ±0.03	12.3 ±0.5			95%			Gri63
1602+178	16 02 53.93	+17 51 57.5	C	E(D)	0.45	57	171± 7	29
PK1602+178	53.93 ±0.03	53.4 ±0.4			100%			Goo79
1710+156	17 10 11.50	+15 39 38.0	C	E	0.23	7	169± 9	30
MLO1710+156	11.52 ±0.02	39.2 ±0.4			(100%)			Pal80
1743+666	17 43 56.73	+66 39 24.9	C	D	0.23	50	65± 3	
WK386	57.59 ±0.06	23.9 ±0.3			100%			Goo79
1833+653	18 33 33.50	+65 19 12.0	C	D(E)	1.36	11	19±12	31
3C383	33.42 ±0.09	12.6 ±0.6			(89%)			Ver75
1940+504	19 40 25.62 ±0.02	+50 28 37.5 ±0.2	S	C(T)	1.34	95	16±10	15,32
3CR402S	25.57 ±0.05	38.2 ±0.4			64%			Pal80
2103+124	21 03 47.70 ±0.03	+12 27 52.4 ±0.3	S	T	0.94	120	138± 3	
PK2103+12	47.73 ±0.04	52.1 ±0.9			96%			Pal80
2322−123	23 22 43.62 ±0.03	−12 23 55.1 ±1.1	S	C	0.91	7	2± 8	
PK2322−12	43.72 ±0.03	56.4 ±0.5			(93%)			Gri63
2354+471	23 54 56.90	+47 09 42.0	C	D	0.99	220	64± 2	33
4C47.63	57.50 ±0.06	39.8 ±0.4			100%			Pal80

Notes to Table I

1. An optical position accurate to approximately 12 arcsec was given by Bolton *et al.* (1968): $00^h38^m17^s.0$, $+08°37'30''$.
2. There may be a bridge of emission along position angle 3° ± 5° connecting the main components.
3. The radio map by itself suggests a bend angle of 50° to 55° for this source, but the placement of the optical identification implies that the bend angle is closer to 35°. The emission near the identification is extended ~30 arcsec.
4. An optical position accurate to approximately 12 arcsec was given by Merkelijn (1969): $02^h17^m24^s.7$, $+01°42'10''$. The radio emission to the 10% contour level extends to ~95 arcsec, but most of the emission is within the quoted LAS.
5. This source is Z-shaped overall and may contain a radio jet. The radio position angle was measured along the bridge of emission (or jet) that connects the outer components.
6. The source has large-scale structure towards its preceding (Western) edge. The LAS may be as large as 150 arcsec. Fomalont (1971), however, shows the source to be barely resolved at 1.4 GHz and estimates a size of 80 arcsec, more consistent with that given here.
7. The map of this source shown here indicates a structure whose LAS and/or position angle differ from those used by PBFB.
8. No contour plot is shown in this paper (see Sec. II).
9. The overall structure and position angle obtained from our 2.7-GHz data agree with the 1.4-GHz results of Fomalont (1971).
10. The structure is barely resolved at 408 MHz by Schilizzi and McAdam (1975).
11. The source is an asymmetric double with a 2:1 ratio of component intensities and a 4:1 ratio of component sizes at 2.7 GHz; its LAS is therefore poorly defined.
12. The source may have an overall Z symmetry. The quoted position angle has been measured along the bright ridge of emission defining the symmetry axis.
13. Maps at both 2.7 and 8.1 GHz are shown in Fig. 2 (see Sec. II).
14. The 2.7-GHz map suggests that there may be an inner region of emission lying along a position angle of 50°.
15. The LAS and/or position angle were measured from a new map made after subtraction of a small-diameter component and have consequently been revised from those used by PBFB.
16. This source contains an extended central component (67 ± 5 mJy at 2.7 GHz and 41 ± 4 mJy at 8.1 GHz) whose diameter is ~5 arcsec in the North-South direction. An 8.1-GHz map of the central source suggests that it contains two roughly equal subcomponents; the centroid of this central component is at $10^h33^m31^s.98$, $+00°21'38''.5$.
17. A small-diameter component at $11^h15^m52^s.54 \pm 0^s.4$, $+31°31'41''.9 \pm 0''.5$ was marginally detected at 8.1 GHz only, as discussed in Paper III, notes to Table I.
18. Most of the emission is within the 46-arcsec LAS used by PBFB, but the LAS quoted here gives greater weight to the outer components visible on the 2.7-GHz map shown in Fig. 3.
19. There is low-level emission out to ~120 arcsec, but most of the emission comes from within the quoted LAS.
20. The quoted LAS takes account of large-scale structure surrounding the component peaks but not represented in the 2.7-GHz map in Fig. 4.
21. Our 8.1-GHz data show a 15 ± 7-mJy small-diameter (<2-arcsec) component at $12^h47^m01^s.65 \pm 0^s.05$, $+50°21'11''.8 \pm 1''.4$ which is not separable from the larger-scale emission at 2.7 GHz. An upper limit of 30 mJy can be placed on the flux density of this component at 2.7 GHz. The 8.1-GHz map in Fig. 4 was made using data from spacings shorter than 900 m, which contain the most information on the structure of the source.
22. A 39-mJy (at 2.7 GHz) confusing source at $13^h03^m13^s.0$, $+36°42'27''$ was subtracted from the data before mapping.
23. The 408-MHz map by Schilizzi and McAdam (1975) does not clearly separate the Western (preceding) component in the radio structure (see Sec. III). The overall bend angle is ~35° and the radio position angle has been measured between the outer radio components. The central component at $14^h07^m34^s.6 \pm 0^s.4$, $14°46'52'' \pm 2''$ is approximately 25 arcsec in diameter.
24. The map shown here supersedes that used by PBFB. This map shows that the source is not well collimated and that its overall position angle is poorly defined.
25. The map by Fomalont (1971) at 1.4 GHz contains a higher percentage of the integrated flux at that frequency than does our map at 2.7 GHz. This source is frequently denoted as 3C296 but lies 2.5° North of the position given by Bennett (1962). An unpublished 2.7-GHz map by Laing (private communication) using the Cambridge 5-km telescope shows a twin jet structure linking the identification to the extended lobes.
26. The radio structure shown in our 2.7-GHz map (Fig. 5) is in good agreement with the 5-GHz map by Fanti *et al.* (1977).
27. Since preparation of Table I, our attention has been drawn to an optical position $14^h49^m51^s.23$, $-12°58'59''.2$ accurate to ~0.5 arcsec given by Schilizzi (1975). A 220-mJy confusing source at $14^h50^m13^s.2$, $-13°07'11''$ was subtracted from the data before mapping. The map shown by Fomalont (1971) has a much larger field of view than our map in Fig. 5 and includes the confusing source.
28. Our 8.1-GHz data show a 20 ± 5-mJy emission peak at $15^h59^m55^s.58 \pm 0^s.04$, $+02°06'14''.8 \pm 0''.6$ which is not separable from the larger-scale structure at 2.7 GHz. An upper limit of 60 mJy can be placed on the 2.7-GHz flux density of any small-diameter (<1-arcsec) component at this position, which is near to, but not coincident with, that of the optical identification. A 408-MHz map by Schilizzi and McAdam (1975) includes a confusing source to the North-West.
29. Jaffe and Perola (1974) show a 5-GHz map superimposed on a photograph of the optical identification. The LAS used in PBFB was measured from an unpublished map by F. N. Owen and L. Rudnick.
30. The placement of the optical identification suggests that this may be a small "head-tail" radio structure.
31. The relatively large error in the position angle is a consequence of the 30° bend angle of this source.
32. The 2.7-GHz map in Fig. 7 and the entries in the table refer only to the radio emission near the Southern galaxy in the structure of 3C402 (see Sec. III). The entire field of 3C402 has been mapped by Miley and van der Laan (1973) at 1.4 GHz and by Riley and Pooley (1975) at 5 GHz.
33. Burns and Owen (1979) show a high-resolution 2.7-GHz map.

Table I references: Ghi77 = Ghigo (1977); Goo79 = Goodson *et al.* (1979) (Paper III); Gri63 = Griffin (1963); Mer70 = Merkelijn and Wall (1970); Pal80 = Palimaka *et al.* (1980) (Paper V); unpub = position estimated from *Palomar Sky Atlas* using an overlay; Ver66 = Véron (1966); Ver75 = Véron and Véron (1975); Wil73 = Wills *et al.* (1973); Wil76 = Wills (1976).

integrated flux density that is contained in a set of Gaussian components fitted to the visibility data which were used to produce the map of the source. Any deficiency below 100% indicates the fraction of the total flux density which may be contained in large-scale structure that is not displayed in the map. If the sum of the flux densities in the fitted components exceeded the integrated flux density, an entry of 100% was placed in the table since such formal excesses are not directly related to intrinsic properties of the sources. When the 8.1-GHz map is shown in Figs. 1 to 7, the lower line of column 6 gives (in parentheses) the ratio to the 2.7-GHz integrated flux density of the 2.7-GHz fringe amplitude at the (u,v) spacing which produced the maximum 8.1-GHz fringe amplitude. This ratio should be used as above to indicate the flux density, if any, missing from the 8.1-GHz map.

Column 7 gives an estimate of the largest angular size (LAS) of the radio source. This was usually measured between the outermost limits of the 20% contour levels on the map of the source shown in Figs. 1 to 7. This LAS is a partly subjective measure of the overall size of the extended radio structure, as discussed in Paper III, Sec. II. The finite resolution of the synthesized beam has been

TABLE II. Radio parameters of confirmed small-diameter components.

SOURCE NAME	R.A. (1950.0)	DEC.	S(2.7) Jy	S(8.1) Jy	DIAMETER arcsec	%FLUX	NOTES
0238+085	$02^h38^m26^s.01 \pm 0^s.18$	$+08°31'26''.8 \pm 1''.2$	0.110 ±0.010	0.040 ±0.010	~4	13.8	1
0305+039	03 05 49.08 ±0.03	+03 55 13.5 ±0.4	1.000 ±0.050	0.800 ±0.070	<0.5	19.6	
0325+023	03 25 18.16 ±0.02	+02 23 20.7 ±0.3	0.140 ±0.010	0.185 ±0.015	<0.5	4.7	
1005+007	10 05 37.34 ±0.03	+00 44 42.5 ±0.4	0.064 ±0.007	0.055 ±0.006	<0.5	18.8	
1154−038	11 54 14.78 ±0.04	−03 48 59.3 ±0.6	0.058 ±0.005	0.052 ±0.005	<1	19.3	
1216+061	12 16 50.00 ±0.03	+06 06 08.4 ±0.3	0.247 ±0.010	0.275 ±0.020	<0.5	2.0	
1250−102	12 50 30.70 ±0.05	−10 13 20.5 ±2.0	0.120 ±0.020	0.040 ±0.010	≤3	18.8	2
1414+110	14 14 26.36 ±0.03	+11 02 18.6 ±0.3	0.057 ±0.005	0.100 ±0.008	<0.5	2.1	
1422+268	14 22 26.51 ±0.04	+26 51 02.3 ±0.5	<0.010	0.020 ±0.004	<2	<2.0	3
1514+004	15 14 06.70 ±0.04	+00 26 01.7 ±0.7	0.530 ±0.030	0.650 ±0.050	<0.5	29.4	
1514+072	15 14 17.01 ±0.02	+07 12 16.6 ±0.5	0.422 ±0.010	0.230 ±0.010	<0.5	20.3	
1940+504	19 40 25.62 ±0.02	+50 28 37.5 ±0.2	0.043 ±0.010	0.023 ±0.005	<1	3.2	4
2103+124	21 03 47.70 ±0.03	+12 27 52.4 ±0.3	0.125 ±0.020	0.150 ±0.020	<0.5	13.3	5
2322−123	23 22 43.62 ±0.03	−12 23 55.1 ±1.1	0.050 ±0.018	0.027 ±0.011	<0.5	5.5	6
Additional small-diameter components from papers III and V:							
0704+351	07 04 24.43 ±0.04	+35 08 24.0 ±0.5	0.035 ±0.013	0.026 ±0.004	~4	10.9	7
1130−037	11 30 31.97 ±0.05	−03 44 12.0 ±1.6	0.056 ±0.006	0.036 ±0.005	~1	11.9	8
1547+309	15 47 11.97 ±0.02	+30 56 21.7 ±0.2	0.237 ±0.010	0.118 ±0.025	~3.5	38.2	9
1615+324	16 15 46.97 ±0.02	+32 29 50.3 ±0.4	0.060 ±0.025	0.015 ±0.006	<4	4.1	10

Notes

1. The core is extended and may be as large as 6 arcsec in diameter. From the data on the 35-km baselines, ~60 mJy is in structure <0.5 arcsec at 2.7 GHz. The peak of emission on an 8.1-GHz map made from the long-baseline data is at $02^h38^m25^s.89 \pm 0^s.04$, $+08°31'28''.6 \pm 0''.6$, which is in good agreement with the optical position measured for the galaxy.
2. The core may have some structure up to 5 arcsec in extent. 60 mJy remain unresolved at the 35-km baselines at 2.7 GHz.
3. The small-diameter component is confirmed by Fanti *et al.* (1977), who find a 20-mJy component at $14^h22^m26^s.5$, 26°51′00″ at 5 GHz. This position is consistent with our small-diameter component position since their beam size is 16 × 8 arcsec.
4. Data on this small-diameter component were also presented in Paper I.
5. There is 70 mJy at 2.7 GHz and 30 mJy at 8.1 GHz in larger-scale (~4-arcsec) emission around a core which is unresolved (<0.5 arcsec) at the 35-km baselines.
6. The 2.7-GHz flux density is estimated from 35-km baseline visibility data. Since the LAS of this source is only ~7 arcsec, the core is barely separable from the rest of the source structure at 8.1 GHz.
7. The 8.1-GHz flux density of this small-diameter component is taken from Rudnick and Owen (1977), who find its 2.7-GHz flux density to be 39 ± 8 mJy, in agreement with our measurement in column 4.
8. The 8.1-GHz flux density has been estimated from a map made from the long-baseline visibility data. The large error in declination is due to incomplete (u,v) coverage.
9. Rudnick and Adams (1979) find the 8.1-GHz flux density of this small-diameter component to be 110 ± 6 mJy.
10. The position of this small-diameter component is taken from Riley and Pooley (1975), who find its 5-GHz flux density to be 26 ± 6 mJy.

taken into account when determining the LAS. If a small-diameter component was detected, the LAS was usually measured from a map on which this component had been removed, in order that the LAS of the extended structures be more uniformly determined.

Column 8 gives the position angle of the major axis (maximum elongation) of the extended radio structure. For simple sources whose extended emission can be well represented by a small number of Gaussian components, these position angles and their errors were determined from the positions and errors of the fitted Gaussian components. For more complex structures the position angles were measured directly from the contour maps and their errors were obtained from a subjective judgment of the uncertainties in defining the position angle of the major axis of the source from the map. The upper line in column 9 gives references to notes on individual sources following the table; the lower line gives a refer-

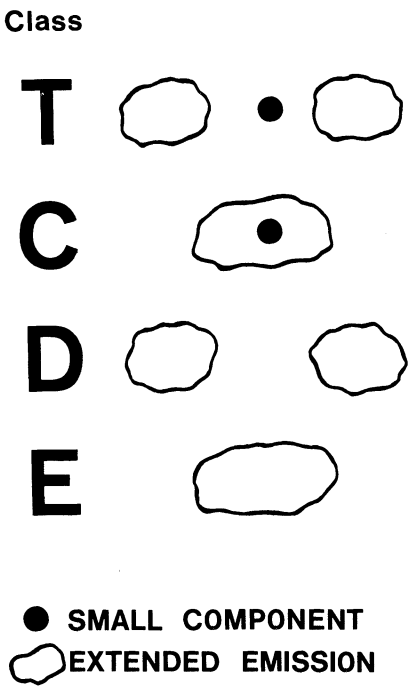

FIG. 8. Key to the classifications of radio structure that are used in Table I, column 5.

ence to the measurement of the optical position of the center of the galaxy proposed as the identification.

Table II presents the radio parameters of small-diameter (<4-arcsec) components that were detected within the extended structures. Columns 2 and 3 repeat the 1950.0 positions of these components from Table I. Columns 4 and 5 list the 2.7- and 8.1-GHz flux densities found either by fitting a point component to the long-spacing interferometer data or, if the small-diameter component is not well separated from the rest of the structure, by modeling the entire structure with a set of Gaussian components which included the small-diameter component. Column 6 gives an estimate of the diameter of the component (FWHM); estimates of <0.5 arcsec were derived from observations over the 35-km baselines (as in Paper I). Column 7 gives the percentage of the integrated flux of the source that is contained in the small-diameter component at 2.7 GHz. Column 8 gives a key to notes on individual small-diameter components.

III. REMARKS ON INDIVIDUAL SOURCES

0238+085 and 1250−102. Both sources have extended radio cores (Table II) indicating that there is fine-scale structure larger than a few arcseconds near their parent galaxies. Both sources also have elongated bridges of emission which connect their cores with the outer radio lobes. There may be two-sided "jets" in these sources similar to those previously observed in 3C31 (Burch 1977; Fomalont *et al.* 1980), NGC 315 (Bridle *et al.* 1979), and 3C449 (Perley *et al.* 1979). 0238+085, in particular, is similar to NGC 315 in that it has a Z-shaped structure which could be interpreted as evidence for precession of the source of a beam transporting energy to the radio lobes. The optical identification of this source has several nearby companions (Paper V), as do other radio galaxies whose structures suggest the presence of precessing beams (Bridle *et al.* 1976; Ekers *et al.* 1978).

1407+177. Our map of this source (Fig. 5) and the map shown by Schilizzi and McAdam (1975) are superficially dissimilar but in fact agree with respect to component positions. The lower resolution of the 408-MHz map by Schilizzi and McAdam does not separate the extended central component shown in our 2.7-GHz map from the Western (preceding) component. The Eastern (following) component has a steep spectrum ($\alpha \sim 1.2$) and is not as dominant at 2.7 GHz as it appears to be at 408 MHz.

1940+504. Data on the small-diameter core within this source were previously given in Paper I. The map shown in Fig. 7 covers only part of the field of 3C402 and was produced by removing the components of 3C402 which are most likely to be associated with the brightest galaxy in the field (VV8-36-2). The elongation and brightness contrast of the components shown suggest

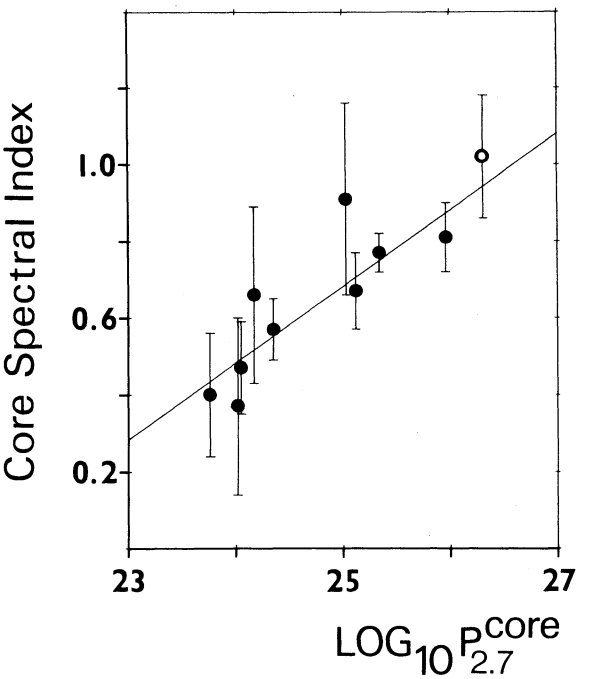

FIG. 9. Spectrum-luminosity correlation for the extended cores (●) and for one example of lobe fine structure (○). The uncertainties in $\log_{10}P_{2.7}$ are <0.1. The least-squares linear regression line of α on $\log_{10}P_{2.7}$ is also shown; in determining this line, we weighted the data inversely as the squares of the uncertainties in α and neglected the errors in $\log_{10}P_{2.7}$. The sources plotted are: 0704+351, 1003+351, 1130−037, 1346+268, 1350+316, 1502+262, 1511+263, 1514+072, 1547+309 (extended cores), and 1420+198 (lobe fine structure).

that they are all associated with the small-diameter core in the galaxy VV8-36-3. The surrounding radio structure is best shown on the map by Miley and van der Laan (1973).

IV. THE SPECTRUM-LUMINOSITY RELATION FOR EXTENDED RADIO CORES

Two of us found in Paper I (Bridle and Fomalont 1978) that the core components in extended radio galaxies are of two kinds—compact cores with 2.7–8.1-GHz spectral indices <0.4 and linear sizes ≪1 kpc, and extended cores with spectral indices >0.4 and linear sizes typically of several kiloparsecs. VLBI observations of some quasars (e.g., Wilkinson *et al.* 1977 and Readhead *et al.* 1979) and VLA studies of low-luminosity radio galaxies (e.g., Bridle *et al.* 1979 and Fomalont *et al.* 1980) have found one-sided jetlike features with spectral indices >0.4 within a few kiloparsecs of several compact cores. These kiloparsec-scale jet features would be classified as extended cores if (a) they were observed at the same relative resolution as the sources studied here and (b) they were not dominated by compact core components. These similarities of scale and spectral index between the bright bases of jets and the extended cores reinforce the suggestion made in Paper I that the kiloparsec-scale extended cores are associated with the energy-transfer and collimation processes in radio galaxies rather than with the primary energy release.

In Paper I two of us showed that the ten extended cores then known to us exhibited a statistically significant correlation between spectral index and luminosity analogous to, but steeper than, the well-known spectrum-luminosity relation for radio galaxies with power-law integrated spectra. We have reinvestigated this correlation using the further data on extended cores contained in Table II.

If the data for all 23 cores in our sample which have 2.7–8.1-GHz spectral indices >0.4 or angular diameters >1 arcsec are combined, the resulting correlation diagram is weakened by the uncertainties in the spectral indices for the weaker or confused cores. Figure 9 shows the spectrum-luminosity relation for the nine extended cores (closed circles) and one example of lobe fine structure (open circle) for which our two-frequency observations define the spectral index with (1σ) uncertainty <0.25. These better-defined spectra confirm the existence of a spectrum-luminosity correlation for the extended cores, which can be fitted by the relation

$$\alpha = (0.0199 \pm 0.015)\log_{10}P_{2.7} - (4.29 \pm 0.40)$$

with a correlation coefficient of 0.934. As the 99.9% confidence limit for a correlation coefficient obtained from ten data points is $r > 0.872$, the observed correlation is highly significant.

We conclude that the spectrum-luminosity correlation for extended cores is real, and hence that a physical mechanism must exist which causes the electron energy spectra of luminous extended cores to be depleted of higher-energy electrons within a few kiloparsecs of the central energy supply.

This work was partially supported by grants to A.H.B. from the Natural Sciences and Engineering Research Council of Canada and from the Advisory Research Committee of Queen's University.

REFERENCES

Bennett, A. S. (1962). Mem. R. Astron. Soc. **68,** 163.
Bolton, J. G., Shimmins, A. J., and Merkelijn, J. (1968). Aust. J. Phys. **21,** 81.
Bridle, A. H., Davis, M. M., Fomalont, E. B., Willis, A. G., and Strom, R. G. (1979). Astrophys. J. Lett. **228,** L9.
Bridle, A. H., Davis, M. M., Meloy, D. A., Fomalont, E. B., Strom, R. G., and Willis, A. G. (1976). Nature **262,** 179.
Bridle, A. H., and Fomalont, E. B. (1978). Astron. J. **83,** 704 (Paper I).
Burch, S. F. (1977). Mon. Not. R. Astron. Soc. **181,** 599.
Burns, J. O., and Owen, F. N. (1979). Astron. J. **84,** 1478.
Ekers, R. D., Fanti, R., Lari, C., and Parma, P. (1978). Nature **276,** 588.
Fanti, C., Fanti, R., Gioia, I. M., Lari, C., Parma, P., and Ulrich, M. H. (1977). Astron. Astrophys. Suppl. **29,** 279.
Fomalont, E. B. (1971). Astron. J. **76,** 513.
Fomalont, E. B., Bridle, A. H., Willis, A. G., and Perley, R. A. (1980). Astrophys. J. **237,** 418.
Ghigo, F. D. (1977). Astrophys. J. Suppl. **35,** 359.
Goodson, R. E., Palimaka, J. J., and Bridle, A. H. (1979). Astron. J. **84,** 1111 (Paper III).
Griffin, R. F. (1963). Astron. J. **68,** 421.
Laing, R. A. Private communication.
Jaffe, W., and Perola, G. C. (1974). Astron. Astrophys. **31,** 223.
Kesteven, M. J. L., and Bridle, A. H. (1977). J. R. Astron. Soc. Can. **71,** 21.
Merkelijn, J. K. (1969). Aust. J. Phys. **22,** 237.
Merkelijn, J. K., and Wall, J. V. (1970). Aust. J. Phys. **23,** 575.
Miley, G. K., and van der Laan, H. (1973). Astron. Astrophys. **28,** 359.
Palimaka, J. J., Bridle, A. H., and Fomalont, E. B. (1980). Astron. J. **85,** 995 (Paper V, following paper).
Palimaka, J. J., Bridle, A. H., Fomalont, E. B., and Brandie, G. W. (1979). Astrophys. J. Lett. **231,** L7.
Perley, R. A., Willis, A. G., and Scott, J. S. (1979). Nature **281,** 437.
Readhead, A. C. S., Pearson, T. J., Cohen, M. H., Ewing, M. S., and Moffet, A. T. (1979). Astrophys. J. **231,** 299.
Riley, J. M., and Pooley, G. G. (1975). Mem. R. Astron. Soc. **80,** 105.
Rudnick, L., and Adams, M. T. (1979). Astron. J. **84,** 437.
Rudnick, L., and Owen, F. N. (1977). Astron. J. **82,** 1.
Schilizzi, R. T. (1975). Mem. R. Astron. Soc. **79,** 75.
Schilizzi, R. T., and McAdam, W. B. (1975). Mem. R. Astron. Soc. **79,** 1.
Véron, M. P., and Véron, P. (1975). Astron. Astrophys. **42,** 1.
Véron, P. (1966). Astrophys. J. **144,** 861.
Wilkinson, P. N., Readhead, A. C. S., Purcell, G. H., and Anderson, B. (1977). Nature **269,** 764.
Wills, B. J. (1976). Astron. J. **81,** 1031.
Wills, B. J., Wills, D., and Douglas, J. N. (1973). Astron. J. **78,** 521.